Relaxation of $(CS_2)_2^-$ to Its Global Minimum Mediated by Water Molecules: Photoelectron Imaging Study

Terefe Habteyes, Luis Velarde, and Andrei Sanov*

Department of Chemistry, University of Arizona, Tucson, Arizona 85721-0041

Received: July 22, 2008

The coexistence of several isomers of $(CS_2)_2^-$ is examined via photoelectron imaging at 355 and 266 nm. Assisted by theoretical calculations, the bands in the photoelectron spectra are assigned to the $CS_2^-\cdot CS_2$ ion−molecule complex (C_s symmetry, $^2A'$ electronic state) and two covalently bound dimer-anion structures: C_{2v} ($^2B_1$) and D_{2h} ($^2B_{3g}$). The isomer distribution depends sensitively on the ion source conditions, particularly the presence of water in the precursor gas mixture. The intensity variation of the photoelectron bands suggests that the presence of water enhances the formation of the global-minimum C_{2v} ($^2B_1$) structure, particularly relative to the metastable (local-minimum) ion−molecule complex. This trend is rationalized with two assumptions. The first is that the presence of H_2O at the cluster formation stage facilitates the nonadiabatic transitions necessary for reaching the global-minimum dimer-anion equilibrium when starting from the $CS_2^- + CS_2$ asymptote. The second is that the initial clusters formed in the presence of water tend to have, on average, more internal energy, which is needed for overcoming the potential energy barriers separating the metastable equilibria from the global-minimum structure. As the covalent bonds are formed, excess solvent molecules are evaporated from the cluster, giving rise to stable $(CS_2)_2^-$ dimer anions. In the $(CS_2)_n^-$, $n \geq 3$, and $(CS_2)_2^-(H_2O)_m$, $m > 0$, clusters, the population of the covalent-dimer core structures diminishes drastically due to more favorable solvent interactions with the monomer-anion (i.e., CS_2^-) core.

1. Introduction

Solvation generally shifts electronic transition bands via the differential effect on the ground and excited states. In particular, solvation interactions can stabilize metastable species and exert control on photochemical processes by either suppressing or completely closing electron photodetachment channels, while enabling, instead, anionic photodissociation pathways. In addition to these well-known effects, the present work demonstrates the intriguing role of water in mediating the intermolecular interactions that lead to the formation of the global-minimum structure of $(CS_2)_2^-$.

Negative ions based on carbon disulfide have diverse electronic structural properties. Although CS_2 is isovalent with CO_2 and has no permanent dipole moment, its polarizability (8.86 Å^3) is about 3 times that of CO_2 (2.911 Å^3).[1] The two molecules are characterized by opposite-sign quadrupole moments: 1.8×10^{-26} esu·cm^2 for CS_2 and -4.3×10^{-26} esu·cm^2 for CO_2.[2] The positive adiabatic electron affinity (EA) of CS_2 (EA = 0.89 ± 0.02 eV)[3] is in contrast to the negative EA of CO_2 (EA = −0.6 ± 0.2 eV).[4] Despite this difference, the vertical detachment energies (VDEs) of the corresponding anions are quite similar (VDE = 1.4 eV for CO_2^- and 1.46 eV for CS_2^-),[5,6] reflecting the bent equilibrium structures of the anions compared to the linear geometries of the neutrals.

The geometric and electronic structures of $(CS_2)_2^-$ have been the focus of numerous experimental and theoretical studies.[5−15] The similarity of the photoelectron spectra of CS_2^- and $(CS_2)_2^-$ at the 2.54 eV photon energy and the small magnitude of the dissociation energy (0.176 ± 0.025 eV) led Bowen and Eaton to suggest an ion−molecule complex, $CS_2^-\cdot CS_2$, structure for the dimer anion.[5] In the gas phase clustering reaction experiments of Hiraoka et al., the dissociation energy of $(CS_2)_2^-$ was discussed in terms of the four-membered-ring, C_{2v} symmetry $C_2S_4^-$ structure, corresponding to the $^2B_1$ electronic state, contrasting the C_s ($^2A'$) ion−molecule complex structure of $CS_2^-\cdot CS_2$.[7] The photoelectron spectroscopy experiment of Tsukuda et al. confirmed the coexistence of the ion−molecule complex and the C_{2v} ($^2B_1$) covalent structure.[6] Their results also showed that the relative intensity of the band corresponding to the covalent structure(s) increases at a higher stagnation pressure in the ion source. The covalent dimer structure was also considered by Maeyama et al. in their interpretation of $(CS_2)_2^-$ photodissociation into $CS_2^- + CS_2$ and $C_2S_2^- + S_2$.[8] An MP2/6-31+G(d) theoretical investigation revealed several additional possible structures, of which two of the most stable ones were nearly degenerate, corresponding to the C_{2v} symmetry $^2B_1$ and $^2B_2$ electronic states.[9] Using B3LYP/6-31+G(d) calculations, Zhang et al.[10] later found that the C_{2v} ($^2B_2$) structure converts to a higher-symmetry D_{2h} geometry ($^2B_{3g}$ electronic state) and claimed the D_{2h} ($^2B_{3g}$) structure to be more stable than the C_{2v} ($^2B_1$).[10]

Amid this controversy, the photoelectron imaging study by our group emphasized the distinct electronic-structural properties of the covalent dimer anions of CO_2 and CS_2.[12,13] Yu et al. recorded infrared spectra of the dimer anion formed by high-frequency discharge in CS_2 and trapped in solid neon and argon.[14] Using the MP2/6-311+G(d) and B3LYP/6-311+G(d) predictions to aid the spectroscopic assignment, they identified a D_{2h} ($^2B_{3g}$) covalent structure as the only electronic ground state of $(CS_2)_2^-$, whose calculated vibrational frequencies matched the observed spectral features.

The diverse, not always consistent findings of the previous experimental studies seem to indicate that the electronic and geometric structures and, therefore, the photochemical properties of $(CS_2)_2^-$ are dependent on its environment and the intermolecular interactions involved. In this work, we investigate the

10.1021/jp806478g CCC: $40.75
Published on Web 09/20/2008

effects of solvation and water-mediated interactions on the CS_2^- and $(CS_2)_2^-$ anions. Using photoelectron imaging, we elucidate the coexistence of several isomers of $(CS_2)_2^-$ and the corresponding larger cluster anions. The ion source conditions, particularly the presence of water in the precursor gas delivery line, are shown to have a pronounced effect on the observed isomer distribution, even for $(CS_2)_2^-$ (which itself contains no water molecules).

2. Experimental Arrangement

The experiments are carried out using the tandem time-of-flight mass spectrometer coupled with a photoelectron imaging assembly, described in detail elsewhere.[16,17] Neutral clusters of CS_2 are formed by passing Ar carrier gas at 40 psi backing pressure over a room-temperature carbon disulfide liquid sample. The CS_2/Ar mixture is expanded through a 0.8 mm orifice pulsed supersonic nozzle (General Valve series 99) into a vacuum chamber with a base pressure of 2×10^{-7} Torr. A continuous electron beam (~1 keV kinetic energy) crosses the supersonic expansion ~4 mm downstream from the nozzle orifice. The $(CS_2)_n^-$ anion clusters are formed by secondary electron attachment to the neutral clusters. The $(CS_2)_2^-(H_2O)_m$ clusters are formed through the same procedure in the presence of water vapor in the precursor gas mixture.

A transverse pulsed electric field (~1 kV over 15 cm) is applied 18 cm downstream from the supersonic valve, extracting the anions into the 2.3 m long flight tube of a Wiley-McLaren time-of-flight mass spectrometer, where they are further accelerated to a kinetic energy of about 3 keV. After passing through a set of ion-optics components, the ions are brought to a temporal and spatial focus in the detection region of the instrument (base pressure 5×10^{-9} Torr). The ions are detected with an in-line microchannel plate detector mounted at the end of the flight tube.

In the subsequent discussion, the term "dry source conditions" refers to the experimental regime where moisture in the neutral precursor gas expansion line has been removed as much as possible by means of baking and pumping. Otherwise, the experiments are referred to as performed under "wet source conditions". Figure 1 displays the representative mass spectra of the cluster anions generated under the two regimes. The spectrum acquired under the wet source conditions shows intense $(CS_2)_n^-(H_2O)_m$ peaks, while only $(CS_2)_n^-$ peaks are prominent under the dry conditions.

Photoelectrons detached from the mass-selected cluster anions with a pulsed, linearly polarized laser beam are accelerated in the direction perpendicular to the ion and laser beam propagation directions following the velocity-map[18] imaging[19,20] procedure. In this work, the photoelectron images are acquired using the 532, 355, and 266 nm output of a Nd:YAG laser (Spectra Physics Laboratory 130-50). The images are typically accumulated over 25 000−100 000 photodetachment events.

3. Results and Analysis

3.1. Homogeneous and Heterogeneous Solvation of CS_2^-. The 355 nm photoelectron images of $(CS_2)_n^-$, $n = 1-4$; $CS_2^-(CO_2)_m$, $m = 1-3$; and $CS_2^-(H_2O)_m$, $m = 1-3$, are shown in parts a, b, and c, respectively, of Figure 2. These and all other photoelectron images presented in this work are recorded with the laser polarization axis set vertical in the figure plane. The photoelectron spectra are extracted from the images via the inverse Abel transformation using the Basis Set Expansion program of Reisler and co-workers.[21]

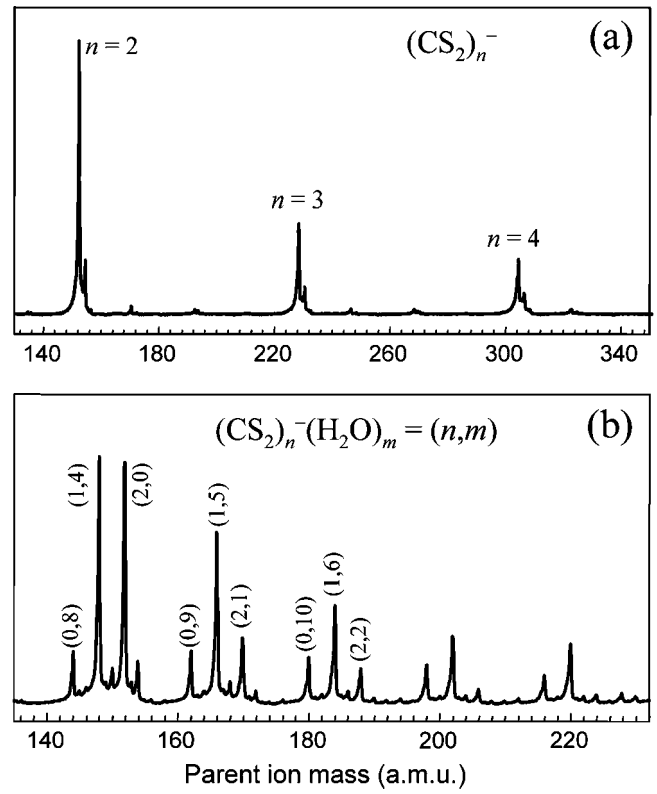

Figure 1. Representative parent-ion mass spectra acquired under (a) dry and (b) wet source conditions, respectively, as described in the text.

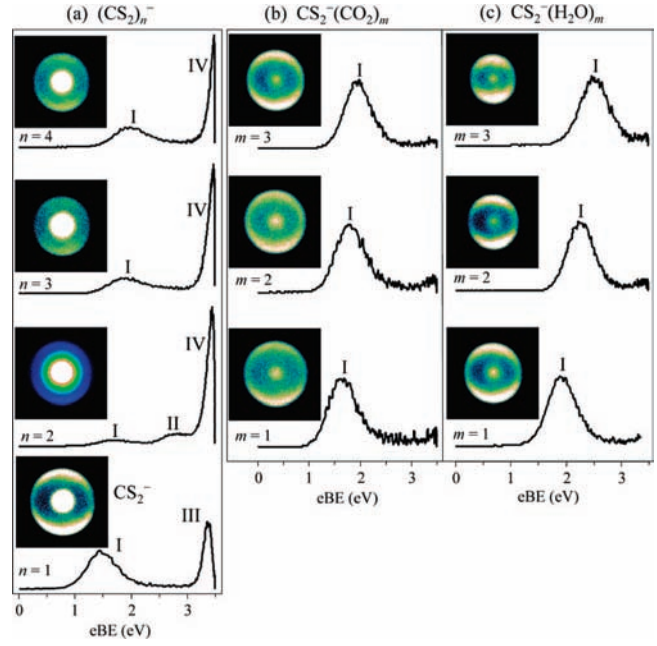

Figure 2. Photoelectron images of isolated and solvated CS_2^- acquired at 355 nm. The laser polarization is always vertical in the image plane. The results for the homogeneous solvation in (a) and heterogeneous solvation in (b) and (c) are shown together for comparison. Band I is assigned to the $X^1A_1(^1\Sigma_g^+) \leftarrow X^2A_1$ transition in CS_2^-. Band II, which appears in $(CS_2)_n^-$ but not in $CS_2^-(CO_2)_m$ and $CS_2^-(H_2O)_m$, is assigned to a covalent dimer-anion structure. Band III in the CS_2^- spectrum is due to the $a^3B_2 \leftarrow X^2A_1$ transition. Band IV observed in $(CS_2)_n^-$, $n \geq 2$, is due to autodetachment from the covalent dimer structures.

In all cases shown in Figure 2, the $X^1A_1(^1\Sigma_g^+) \leftarrow X^2A_1$ transition band in CS_2^-, denoted as band I, shifts progressively to higher binding energies upon the addition of solvent

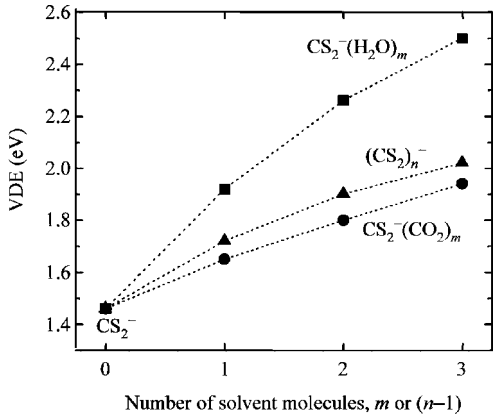

Figure 3. Vertical detachment energy corresponding to band I (see Figure 2) for different types of clusters as a function of number of solvent molecules.

molecules, which is consistent with the energetics of solvation. The solvation-induced shifts observed for band I in the presence of varying numbers of CS_2, CO_2, and H_2O solvent molecules are summarized in Figure 3. Band II, which appears in $(CS_2)_n^-$ (most prominently for $n = 2$), but not in $CS_2^-(CO_2)_m$ and $CS_2^-(H_2O)_m$, is assigned to a covalent structure of $(CS_2)_2^-$, i.e., $C_2S_4^-$. The $a^3B_2 \leftarrow X\ ^2A_1$ transition (band III) is prominent in the low electron kinetic energy (eKE) region of the CS_2^- spectrum, but disappears almost completely upon solvation by CO_2 or H_2O, as seen in Figure 2b,c. Most strikingly, the anion stabilization with the addition of just one, relatively weakly bound CO_2 solvent molecule is enough to make photodetachment band III in solvated CS_2^- practically inaccessible at 355 nm (notice the absence of this band in Figure 2b for $m = 1$, as well as larger m). As seen in Figure 3, the solvation shift of band I due to CS_2 is larger than that due to CO_2. Since a qualitatively similar trend is expected for band III, it should also disappear from the 355 nm spectra upon the addition of the first CS_2 solvent molecule. Therefore, despite its similarity (on a coarse inspection) to band III in CS_2^-, the slow-electron band appearing near the centers of the $(CS_2)_n^-$, $n = 2-4$, images in Figure 2a cannot be due to solvated CS_2^-. We give this band a distinct label: band IV.

In Figure 4, the 355 nm photoelectron spectra of (a) $(CS_2)_n^-$, $n = 2-4$, are compared to those of (b) $(CS_2)_2^-(H_2O)_m$, $m = 0-2$. The results for the two cluster series were obtained under the dry and wet source conditions, respectively. Similar to the data in Figure 2a for $n = 2-4$, all spectra in Figure 4 show intense low-eKE bands (band IV). To provide further evidence that this band is distinct from band III, or other bands attributed to CS_2^-, Figure 4 also shows (as red dotted lines) the photoelectron spectra of $(CS_2)_2^-$ obtained at 266 nm under the corresponding ion-source conditions. It is clear that in $CS_2^-\cdot CS_2$, the $a^3B_2 \leftarrow X^2A_1$ transition responsible for band III appears at binding energies that exceed the 355 nm photon energy.

Since band IV is seen in cluster anions with two or more CS_2 moieties, its likely origin is the covalent dimer anion. Past measurements on $(CS_2)_n^-$, $n = 2-4$, at several wavelengths have also indicated intense, isotropic low-eKE signals,[12,13] similar to band IV. In general, autodetachment bands are quite common in the low-eKE regions of cluster-anion photoelectron spectra. Their origin is traced to the optical preparation and subsequent decay (e.g., via dissociative autodetachment) of excited anionic states. Depending on the energetics and relative cross sections, this process may compete favorably with direct

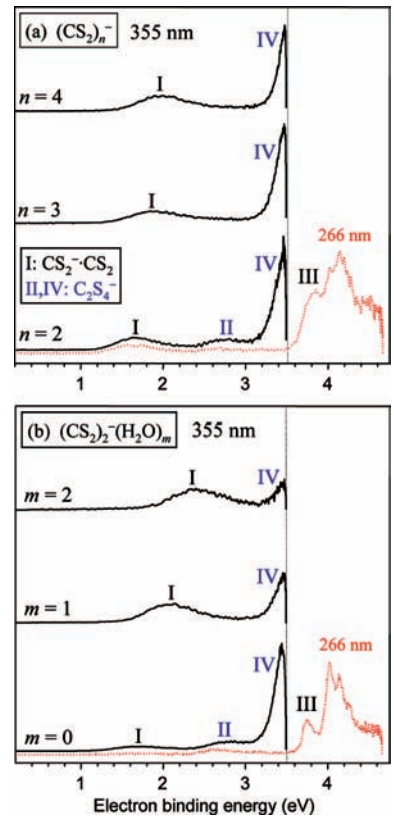

Figure 4. Photoelectron spectra of (a) $(CS_2)_n^-$ and (b) $(CS_2)_2^-(H_2O)_m$ obtained at 355 nm. The 266 nm photoelectron spectrum of $(CS_2)_2^-$ anion is also included as a reference (shown as a red dotted line). As in Figure 2, bands I and II arise from direct photodetachment from $CS_2^-\cdot CS_2$ ion−neutral complex and $C_2S_4^-$ covalent structures, respectively. Band IV is due to $C_2S_4^-$ autodetachment.

photodetachment and photodissociation. A possible origin of band IV is a covalent $C_2S_4^-$ structure with an excited state that decays via (dissociative) autodetachment and/or dissociation (followed by hot fragment autodetachment) at 355 nm. To this end, in the Franck−Condon region the neutral state of the dimer lies below the anionic excited states; therefore, the preparation of these states *should* lead to autodetachment. On the other hand, we have also observed a competing process of the photodissociation of the dimer anion at 355 nm into $CS_2^- + CS_2$ and $C_2S_2^- + S_2$.[22] In Figure 4 the autodetachment signal is suppressed more significantly in the $(CS_2)_2^-(H_2O)_m$, $m \geq 1$, clusters compared to $(CS_2)_n^-$, $n \geq 3$, indicative of the more effective stabilization of the anionic states by H_2O rather than CS_2.

Comparing the relative intensities of bands I and II in Figure 4a for $n = 2$ and Figure 4b for $m = 0$, it can be seen that band I is relatively more intense when $(CS_2)_2^-$ is prepared under the dry source conditions, while band II is more intense under the wet conditions. This observation may appear surprising at first, since the $(CS_2)_2^-$ anion does not include a water moiety. Band II diminishes in intensity upon the addition of either a CS_2 or H_2O solvent molecule to $(CS_2)_2^-$. The band's disappearance could be attributed, in part, to a solvation-induced spectral shift: while band II is expected to move to higher electron binding energies (eBEs) with the addition of solvent molecules, band IV always peaks near eKE = 0. Therefore, in larger clusters band II will eventually overlap with the more intense band IV. However, the projected spectral shift is not sufficient to explain band II's near absence in $(CS_2)_3^-$ and $(CS_2)_2^-\cdot H_2O$. Therefore,

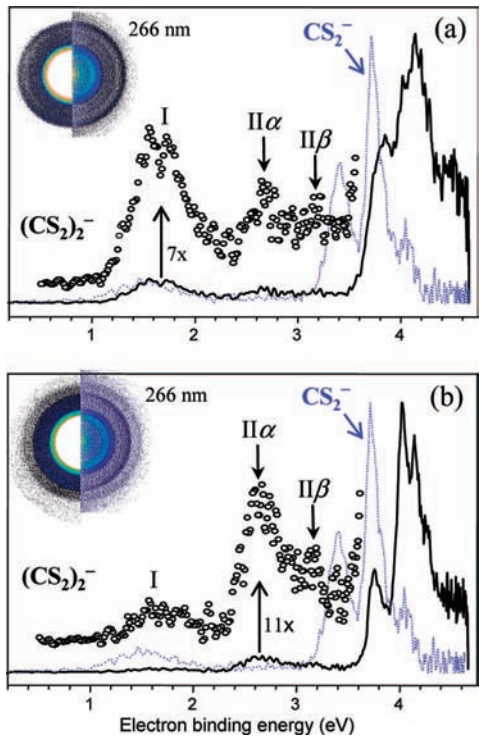

Figure 5. The 266 nm photoelectron images and the corresponding photoelectron spectra of $(CS_2)_2^-$ formed under (a) dry and (b) wet source conditions. Also shown are the magnified portions of the spectra in the electron binding energy range of 0.5−3.5 eV. The photoelectron spectrum of CS_2^- extracted from a 266 nm image is included (dotted line) for reference.

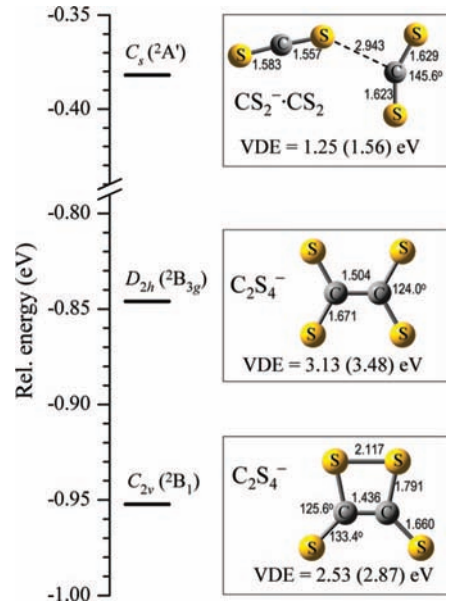

Figure 6. Stable structures of $(CS_2)_2^-$ optimized at the MP2 level with the aug-cc-pVTZ basis set. For each optimized structure, the single point CCSD(T)/6-311+G(3df) energy is calculated relative to the CS_2^- ($^2A_1$) + CS_2 ($^1\Sigma_g^+$) dissociation limit. Bond lengths are shown in angstroms and bond angles are in degrees. The VDEs are calculated using the CCSD(T)/6-311+G(3df) and B3LYP/aug-cc-pVTZ methods are also indicated (with the B3LYP values given in parentheses).

we attribute this band's behavior to a decrease in the relative abundance of the corresponding core-anion isomer(s) in larger clusters.

3.2. $(CS_2)_2^-$: Photoelectron Imaging and Theoretical Calculations. We now turn to $(CS_2)_2^-$, first focusing on its electronic and geometric structures and then considering the sharp, reproducible variations in the isomer population balance depending on the presence of water in the precursor gas delivery line. Figure 5 shows the 266 nm photoelectron images and spectra of $(CS_2)_2^-$ formed under the dry and wet source conditions, respectively. The left and right halves of the images shown represent the raw and Abel-inverted data, respectively.

To facilitate the analysis, the $(CS_2)_2^-$ data are compared to the photoelectron spectrum of CS_2^-, shown in both Figure 5a and Figure 5b by dotted lines. The CS_2^- spectrum is derived from a 266 nm photoelectron image, not included here due to its similarity to the past result.[23] Following the previous studies,[6,23,24] the CS_2^- bands peaking at eBE = 1.46, 3.38, 3.72, and 4.03 eV are assigned to transitions from the X^2A_1 state of CS_2^- to the $X^1A_1(^1\Sigma_g^+)$, a^3B_2, b^3A_2, and A^1A_2 neutral states, respectively. Of these, only the first two transitions were accessible at 355 nm (Figure 2). Under the adopted nomenclature, these two lowest-energy CS_2^- transitions, $X^1A_1(^1\Sigma_g^+) \leftarrow X^2A_1$ and $a^3B_2 \leftarrow X^2A_1$, are responsible for bands I and III, respectively, in the photoelectron spectra presented throughout this paper.

Examining the $(CS_2)_2^-$ spectra in Figure 5 in comparison with the CS_2^- spectrum, the $(CS_2)_2^-$ band centered at eBE = 1.69 eV (band I) is assigned to the CS_2^-·CS_2 ion−molecule complex. This band is shifted by 0.23 eV relative to bare CS_2^-. Band II, assigned to covalent $C_2S_4^-$, exhibits a partially resolved doublet character, which was not clear in the 355 nm results in Figure 2a (presumably due to the overlap with the intense autodetachment transition, band IV). The two components of band II, seen at 266 nm, are labeled in Figure 5 as IIα and IIβ.

To assist the $(CS_2)_2^-$ spectral band assignments, we carried out ab initio and density functional theory (DFT) calculations on the University of Arizona supercomputer using the Gaussian 03 software package.[25] The details of the calculations are described elsewhere.[22] In brief, the geometric structures shown in Figure 6 were obtained by geometry optimizations at the MP2 theory level with the aug-cc-pVTZ basis set. To estimate the VDEs for each isomer, single point energy calculations were performed for the optimized geometries at the CCSD(T)/6-311+G(3df) level of theory. For comparison, the geometry optimizations and VDE calculations were also performed using B3LYP/aug-cc-pVTZ.

As in the previous studies,[6,12,13] the $(CS_2)_2^-$ band at eBE = 2.69 eV (band IIα in Figure 5) is assigned to a $C_2S_4^-$ covalent structure. The location of this band is in reasonable agreement with the VDE estimated for the C_{2v} ($^2B_1$) $C_2S_4^-$ anion based on the CCSD(T)/6-311+G(3df) and B3LYP/aug-cc-pVTZ calculations (2.53 and 2.87 eV, respectively; see Figure 6). The band at 3.17 eV (band IIβ) has not been assigned until recently,[15] although the doublet structure of the spectrum in this spectral region is discernible in the past data.[6] We assign this band to direct photodetachment from the D_{2h} ($^2B_{3g}$) covalent structure shown in Figure 6, as the location of the band's maximum is in good agreement with the VDE values for this structure obtained from both the CCSD(T) (3.13 eV) and B3LYP (3.48 eV) calculations.

A recent report by Matsuyama and Nagata[15] suggested the C_{2v} ($^2B_2$) structure (also discussed previously[9]) as the 3.17 eV band origin. Using DFT calculations, the authors described this structure as a double minimum on the potential energy curve calculated as a function of the SCC angle. The calculations indicated the D_{2h} ($^2B_{3g}$) structure as a transition state between the two symmetric C_{2v} ($^2B_2$) minima.[15] The results of our CCSD(T)/6-311+G(3df)//MP2/6-311+G(3df) calculations con-

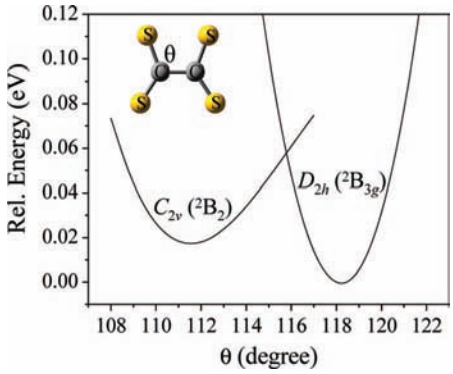

Figure 7. Potential energy curves corresponding to the C_{2v} ($^2B_2$) and D_{2h} ($^2B_{3g}$) structures, calculated as a function of the SCC angle (θ) scanned with a 1° step size. All other degrees of freedom were relaxed, subject to the corresponding symmetry constraints. The geometry optimizations are performed at the MP2/6-311+G(3df) level, followed by single point CCSD(T)/6-311+G(3df) energy calculations.

tradict these DFT predictions. As shown in Figure 7, the CCSD(T)//MP2 calculations indicate that the D_{2h} ($^2B_{3g}$) minimum lies slightly below the C_{2v} ($^2B_2$) structure. Similar discrepancies between the predictions of DFT and ab initio methods in the $(CS_2)_2^-$ case have been observed previously;[22] they may be at least partially responsible for the controversy still surrounding this anion's electronic and geometric structures.[7−10] We have verified that the B3LYP/aug-cc-pVDZ harmonic frequency calculations for the D_{2h} ($^2B_{3g}$) optimized geometry do indeed indicate one imaginary frequency, consistent with this structure's characterization as a transition state between two C_{2v} ($^2B_2$) minima,[15] while the MP2 calculations with the same basis set show no imaginary frequencies.

Considering the zero-point vibrational energy corrections and possible state mixing, the energetic and spectroscopic distinctions between the C_{2v} ($^2B_2$) and D_{2h} ($^2B_{3g}$) dimer-anion structures may in fact be insignificant. A further higher-level theoretical investigation is called for, but one possibility is that the C_{2v} ($^2B_2$)/D_{2h} ($^2B_{3g}$) anion exists in a superposition of two strongly coupled states. With the support from the present CCSD(T)//MP2 calculations, we assign photoelectron band IIβ in Figure 5 to the D_{2h} ($^2B_{3g}$) covalent structure (shown in Figure 6), but the discrepancy with Matsuyama and Nagata's assignment of this band to the C_{2v} ($^2B_2$) structure[15] is possibly trivial, stemming from the deficiencies of the DFT and ab initio models of this very complex system.

3.3. Effect of Hydration on $(CS_2)_2^-$. Even though both data sets in Figure 5 correspond to (nominally) the same anion, there are significant differences between the spectra. The relative band intensity variations reflect the isomer distributions and possibly different anion temperatures, depending on the ion source conditions. Based on the band assignments discussed in section 3.2, the presence of water in the precursor gas mixture enhances the formation of the global-minimum C_{2v} ($^2B_1$) covalent structure relative to $CS_2^-\cdot CS_2$. Figure 5 includes magnified portions of the spectra in the eBE = 0.5−3.5 eV range. Under the dry source conditions (Figure 5a), band I, assigned to $CS_2^-\cdot CS_2$, is more intense than both bands IIα and IIβ, assigned to $C_2S_4^-$. In contrast, under the wet source conditions (Figure 5b), the covalent bands, especially IIα, are markedly more intense than band I.

The unsolvated CS_2^- spectrum included in Figure 5 features three intense partially resolved bands in the range of eBE = 3.2−4.2 eV. These CS_2^- transitions shifted by solvation dominate the eBE ≥ 3.6 eV region of the $(CS_2)_2^-$ spectrum.

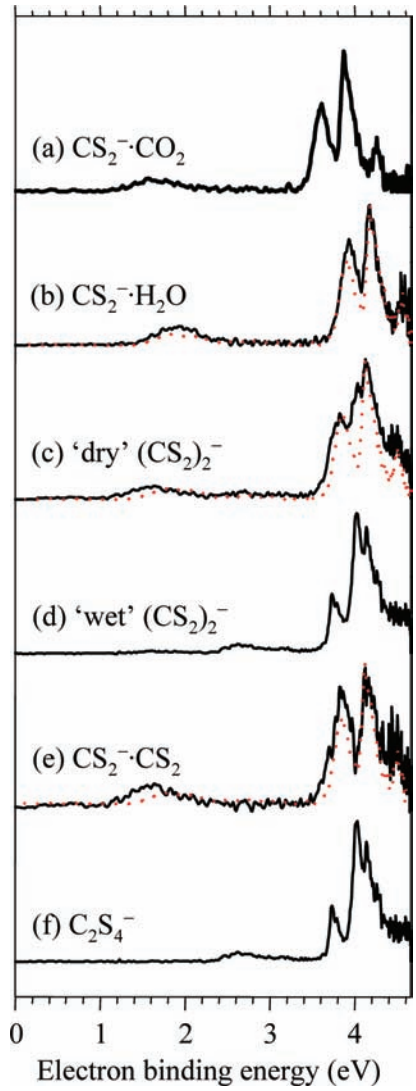

Figure 8. Photoelectron spectra of $(CS_2)_2^-$ and solvated CS_2^- extracted from 266 nm photoelectron images. The dotted lines in (b), (c), and (e) correspond to the shifted $CS_2^-\cdot CO_2$ spectrum from (a). The difference spectra in (e) and (f), corresponding primarily to the $CS_2^-\cdot CS_2$ and $C_2S_4^-$ structures, respectively, were obtained as described in the text.

However, carefully inspecting the $(CS_2)_2^-$ spectra in Figure 5, we observe the presence of additional bands in this region that cannot be ascribed to $CS_2^-\cdot CS_2$. Comparing the spectra in Figure 5a vs 5b, we further note that, similar to bands I and II, the relative intensities of the bands in the eBE > 3.6 eV region depend on the ion source conditions.

To clarify the band assignment in this congested spectral region (eBE ≥ 3.6 eV), we acquired 266 nm photoelectron images of CS_2^- solvated by CO_2, H_2O, and O_2. The spectra for the CO_2 and H_2O solvents are presented in Figure 8a and 8b, respectively (the corresponding spectra for CS_2-O_2 system are available in ref 22). These spectra are compared to the $(CS_2)_2^-$ data obtained under the dry and wet source conditions, shown in Figure 8c and 8d, respectively. Although these $(CS_2)_2^-$ spectra are very similar to the results in Figure 5, they represent different experimental runs under the respective source conditions. The duplicate data sets are shown to demonstrate the reproducibility of the experimental observations.

The motivation for the supplementary measurements presented in Figure 8a,b is that, on the one hand, the $CS_2^-\cdot CO_2$ and $CS_2^-\cdot H_2O$ photoelectron spectra are expected to be affected

by solvation in a manner similar to that of the $CS_2^-\cdot CS_2$ ion−molecule complex. On the other hand, the CO_2 and H_2O molecules are not expected to form favorable covalent bonds with CS_2^-. Hence, by comparing the spectra of $(CS_2)_2^-$ with those of $CS_2^-\cdot CO_2$ and $CS_2^-\cdot H_2O$, it should be possible to identify the signatures of the covalent dimer anion in the congested $(CS_2)_2^-$ spectra.

As seen in Figure 8a,b, the three characteristic CS_2^- bands at eBE > 3.2 eV remain resolved upon solvation. The overall spectral patterns remain similar despite the difference in the solvation energies for CO_2 and H_2O. To emphasize this point, the $CS_2^-\cdot CO_2$ spectrum, shifted by 0.30 eV to higher energy, is superimposed (dotted line) in Figure 8b with the $CS_2^-\cdot H_2O$ spectrum (solid line). There are no significant differences between the shifted $CS_2^-\cdot CO_2$ and the $CS_2^-\cdot H_2O$ spectra. Similarly, in Figure 8c, the same $CS_2^-\cdot CO_2$ spectrum, shifted by 0.25 eV, is superimposed with the dry- and wet-source $(CS_2)_2^-$ spectra. Now, significant differences can be seen in the band structures. Assuming that the spectral variations are due to changes in the isomer population balance, the analysis of the two spectra allows us to separate them (at least approximately) into the $CS_2^-\cdot CS_2$ and $C_2S_4^-$ contributions.

First, we assume that band II intensity is proportional to the $C_2S_4^-$ population, neglecting for the time being the possible variations in the C_{2v} ($^2B_1$) and D_{2h} ($^2B_{3g}$) relative populations. By normalizing the spectra in Figure 8c,d to the same band II intensity and taking their difference, we expect to obtain a $(CS_2)_2^-$ spectrum, from which the contributions of the covalently bound $C_2S_4^-$ structures have been approximately removed. That is, the difference spectrum shown in Figure 8e is due primarily to the $CS_2^-\cdot CS_2$ ion−molecule complex and indeed it bears a close resemblance to the (shifted) $CS_2^-\cdot CO_2$ and $CS_2^-\cdot H_2O$ spectra. Next, we take advantage of band I's assignment to $CS_2^-\cdot CS_2$. By normalizing the spectra in Figure 8c,d to the same band I intensity and subtracting (c) from (d), we obtain the difference spectrum shown in Figure 8f, which is attributed primarily to the covalent $C_2S_4^-$ structures. Comparing the spectra in (d) and (f), it is apparent that the $(CS_2)_2^-$ spectrum acquired under the wet source conditions is characteristic mainly of the covalent $C_2S_4^-$ structures.

4. Discussion

The results presented in the previous section indicate that the $(CS_2)_2^-$ anion, as well as the larger CS_2-based cluster anions, exists in several isomeric forms. The point-group symmetries (and the corresponding electronic states) of the proposed $(CS_2)_2^-$ structures are C_s ($^2A'$), C_{2v} ($^2B_1$), and D_{2h} ($^2B_{3g}$). The corresponding geometries and relevant energetics are summarized in Figure 6. The coexistence of several isomers for $(CS_2)_2^-$ is in marked contrast with $(CO_2)_2^-$, for which only the covalently bound D_{2d} ($^2A_1$) structure has been observed experimentally.[26]

The presence of water in the precursor gas enhances the formation of cluster isomers that give rise to bands II (particularly IIα). This band is assigned to the most stable covalent dimer structure, C_{2v} ($^2B_1$), while its satellite band IIβ is ascribed to the D_{2h} ($^2B_{3g}$) isomer. Dry source conditions, on the other hand, favor (in relative terms) the formation of the $CS_2^-\cdot CS_2$ ion−molecule complex.

The accepted mechanism of cluster anion formation involves the attachment of slow secondary electrons to neutral clusters in the supersonic expansion,[27] while the resulting anions are stabilized by solvent evaporation. From the electronic structure perspective, the C_s ($^2A'$) structure of $(CS_2)_2^-$, which correlates to the $CS_2^- + CS_2$ dissociation limit, can be thought of as resulting from the addition of an electron to the lowest unoccupied molecular orbital (LUMO) of $(CS_2)_2$ in its ground electronic state, corresponding to the neutral van der Waals dimer. Hence, the formation of the $CS_2^-\cdot CS_2$ ion−molecule complex can be described as straightforward electron capture by neutral clusters, followed by the anion stabilization by solvent evaporation.

On the other hand, at least within the single-reference picture, the electron configurations of the C_{2v} ($^2B_1$) and D_{2h} ($^2B_{3g}$) structures of $(CS_2)_2^-$ are both derived from the electron addition to the "doubly excited" neutral $(CS_2)_2$ species, which can be thought of as resulting from singlet coupling of two CS_2 moieties, individually promoted to their respective triplet states.[9] The electronic states of the C_{2v} ($^2B_1$) and D_{2h} ($^2B_{3g}$) structures do not correlate adiabatically to the $CS_2^-(X\ ^2A_1) + CS_2(X\ ^1\Sigma_g^+)$ dissociation limit or to the C_s ($^2A'$) electronic state of $CS_2^-\cdot CS_2$. Therefore, the formation of these dimer-anion structures by electron addition to van der Waals clusters of CS_2 must proceed via nonadiabatic transitions and potential energy barriers.

The observed variations in the photoelectron spectrum of $(CS_2)_2^-$, depending on the presence of water molecules, can be rationalized with the assumption that *in the absence of water* the newly formed cluster anions are stabilized more efficiently in the local minimum corresponding to the C_s ($^2A'$) $CS_2^-\cdot CS_2$ structure. Initially, we expect the excess electron to enter the LUMO of a CS_2 molecule within the cluster, leading to the straightforward formation of the C_s ($^2A'$) dimer structure. The efficiency of relaxation toward the global-minimum C_{2v} ($^2B_1$) structure depends on at least two factors: the strength of nonadiabatic couplings and the availability of excess energy to overcome the potential energy barriers separating the local and global minima.

Considering the first factor, water molecules induce a greater perturbation on the solute, compared to other solvent molecules, as evidenced, for example, by the photoelectron spectra throughout this paper. Thus, the presence of water may facilitate the nonadiabatic interactions leading to the formation of the global-minimum anionic structure, even if H_2O is evaporated once the ground electronic state is formed. As for the availability of energy, the $(CS_2)_2^-$ anions hydrated by water molecules can be very hot compared to other solvent molecules, as well as Ar atoms present in the precursor supersonic expansion. Higher internal temperatures in the presence of H_2O should facilitate surmounting the potential barriers, enabling the anion relaxation from the initial local minima to the global-minimum structure. The heat released during the formation of the more stable equilibrium may then lead to the evaporation of water, ultimately yielding an unhydrated $C_2S_4^-$ anion.

The temperature effect on cluster structures can be seen in the previously published data as well. In the $(CS_2)_2^-$ photoelectron spectra recorded by Tsukuda et al.,[6] the relative intensity of the bands corresponding to $CS_2^-\cdot CS_2$ was stronger at a higher stagnation pressure of the Ar carrier gas. Although not addressed in the previous work, this effect can be rationalized in view of the above discussion. Namely, the higher stagnation pressure yields a colder cluster environment, where the ions are more effectively trapped at local potential minima. The formation of local minimum structures in "cold" environments has also been demonstrated for other systems, including the $(H_2O)_m^-$, $m \leq 200$, cluster anions by Verlet et al.[28] and the $(H_2O)_6$ neutral cluster by Nauta and Miller.[29]

If water molecules remain present in the cluster, another factor comes into play. The excess electron will then tend to localize on the CS_2 monomer, due to more favorable interaction of H_2O

with the more localized charge distribution of CS_2^-, compared to $C_2S_4^-$. This effect is reflected in Figure 4b, where the relative intensity of the C_{2v} ($^2B_1$) band decreases in the photoelectron spectra of $(CS_2)_2^-(H_2O)_m$ for $m \geq 1$. This also holds true for the homogeneous solvation, as can be seen in Figures 2a and 4a, where the relative intensity of the corresponding band declines similarly in the photoelectron spectra of $(CS_2)_n^-$ for $n > 2$.

5. Summary

The photoelectron imaging results highlight the structural complexity of $(CS_2)_2^-$. Several $(CS_2)_2^-$ isomers are generated in the ion source, with their population distribution depending sensitively on the source conditions, particularly the presence of water vapor in the precursor gas mixture. Based on the assignment of the bands in the photoelectron spectra, the coexistence of the following isomers is proposed for $(CS_2)_2^-$: the $CS_2^-\cdot CS_2$ [C_s ($^2A'$)] ion−molecule complex and two covalent structures, C_{2v} ($^2B_1$) and D_{2h} ($^2B_{3g}$). The presence of water in the precursor gas mixture enhances the formation of the global-minimum C_{2v} ($^2B_1$) structure relative to $CS_2^-\cdot CS_2$. It is proposed that the formation of the global-minimum structure is facilitated by the hydration-induced nonadiabatic interactions and the higher internal temperature expected for the initially formed (metastable) cluster anions containing water molecules. In the equilibration process leading to the C_{2v} ($^2B_1$) cluster core, the solvent molecules tend to evaporate. If some remain within the cluster, their stronger interactions with the more localized charge distribution of CS_2^-, compared to $C_2S_4^-$, favor (energetically) the monomer anion based structures for the $(CS_2)_n^-$, $n > 2$, and $(CS_2)_2^-(H_2O)_m$, $m > 0$, cluster anions.

Acknowledgment. We have benefited greatly from the past published[9] and unpublished discussions of the electronic structure of $(CS_2)_2^-$ with Professor Ken D. Jordan. The financial support for this work is provided by the National Science Foundation (Grant CHE-0713880) and the ACS Petroleum Research Fund (Grant 45406-AC6).

References and Notes

(1) *CRC Handbook of Chemistry and Physics*, 84th ed.; CRC Press: Boca Raton, FL, 2004.
(2) Battaglia, M. R.; Buckingham, A. D.; Neumark, D.; Pierens, R. K.; Williams, J. H. *Mol. Phys.* **1981**, *43*, 1015.
(3) Oakes, J. M.; Ellison, G. B. *Tetrahedron* **1986**, *42*, 6263.
(4) Compton, R. N.; Reinhardt, P. W.; Cooper, C. D. *J. Chem. Phys.* **1975**, *63*, 3821.
(5) Bowen, K. H.; Eaton, J. G. Photodetachment Spectroscopy of Negative Cluster Ions. In *The Structure of Small Molecules and Ions*; Naaman, R., Vager, Z., Eds.; Plenum: New York, 1988; p 147.
(6) Tsukuda, T.; Hirose, T.; Nagata, T. *Chem. Phys. Lett.* **1997**, *279*, 179.
(7) Hiraoka, K.; Fujimaki, S.; Aruga, G.; Yamabe, S. *J. Phys. Chem.* **1994**, *98*, 1802.
(8) Maeyama, T.; Oikawa, T.; Tsumura, T.; Mikami, N. *J. Chem. Phys.* **1998**, *108*, 1368.
(9) Sanov, A.; Lineberger, W. C.; Jordan, K. D. *J. Phys. Chem. A* **1998**, *102*, 2509.
(10) Zhang, S. W.; Zhang, C. G.; Yu, Y. T.; Mao, B. Z.; He, F. C. *Chem. Phys. Lett.* **1999**, *304*, 265.
(11) Koizumi, S.; Yasumatsu, H.; Otani, S.; Kondow, T. *J. Phys. Chem. A* **2002**, *106*, 267.
(12) Mabbs, R.; Surber, E.; Sanov, A. *Analyst* **2003**, *128*, 765.
(13) Mabbs, R.; Surber, E.; Sanov, A. *Chem. Phys. Lett.* **2003**, *381*, 479.
(14) Yu, L. A.; Zeng, A. H.; Xu, Q. A.; Zhou, M. F. *J. Phys. Chem. A* **2004**, *108*, 8264.
(15) Matsuyama, Y.; Nagata, T. *Chem. Phys. Lett.* **2008**, *457*, 31.
(16) Habteyes, T.; Velarde, L.; Sanov, A. *Chem. Phys. Lett.* **2006**, *424*, 268.
(17) Velarde, L.; Habteyes, T.; Sanov, A. *J. Chem. Phys.* **2006**, *125*, 114303.
(18) Eppink, A. T. J. B.; Parker, D. H. *Rev. Sci. Instrum.* **1997**, *68*, 3477.
(19) Chandler, D. W.; Houston, P. L. *J. Chem. Phys.* **1987**, *87*, 1445.
(20) Thoman, J. W.; Chandler, D. W.; Parker, D. H.; Janssen, M. H. M. *Laser Chem.* **1988**, *9*, 27.
(21) Dribinski, V.; Ossadtchi, A.; Mandelshtam, V. A.; Reisler, H. *Rev. Sci. Instrum.* **2002**, *73*, 2634.
(22) Habteyes, T. G. Ph.D. Dissertation, University of Arizona, 2008.
(23) Surber, E.; Mabbs, R.; Sanov, A. *J. Phys. Chem. A* **2003**, *107*, 8215.
(24) Surber, E.; Sanov, A. *J. Chem. Phys.* **2002**, *116*, 5921.
(25) Frisch, M. J.; Trucks, G. W.; Schlegel, H. B.; Scuseria, G. E.; Robb, M. A.; Cheeseman, J. R.; Montgomery, J. A., Jr.; Vreven, T.; Kudin, K. N.; Burant, J. C.; Millam, J. M.; Iyengar, S. S.; Tomasi, J.; Barone, V.; Mennucci, B.; Cossi, M.; Scalmani, G.; Rega, N.; Petersson, G. A.; Nakatsuji, H.; Hada, M.; Ehara, M.; Toyota, K.; Fukuda, R.; Hasegawa, J.; Ishida, M.; Nakajima, T.; Honda, Y.; Kitao, O.; Nakai, H.; Klene, M.; Li, X.; Knox, J. E.; Hratchian, H. P.; Cross, J. B.; Bakken, V.; Adamo, C.; Jaramillo, J.; Gomperts, R.; Stratmann, R. E.; Yazyev, O.; Austin, A. J.; Cammi, R.; Pomelli, C.; Ochterski, J. W.; Ayala, P. Y.; Morokuma, K.; Voth, G. A.; Salvador, P.; Dannenberg, J. J.; Zakrzewski, V. G.; Dapprich, S.; Daniels, A. D.; Strain, M. C.; Farkas, O.; Malick, D. K.; Rabuck, A. D.; Raghavachari, K.; Foresman, J. B.; Ortiz, J. V.; Cui, Q.; Baboul, A. G.; Clifford, S.; Cioslowski, J.; Stefanov, B. B.; Liu, G.; Liashenko, A.; Piskorz, P.; Komaromi, I.; Martin, R. L.; Fox, D. J.; Keith, T.; Al-Laham, M. A.; Peng, C. Y.; Nanayakkara, A.; Challacombe, M.; Gill, P. M. W.; Johnson, B.; Chen, W.; Wong, M. W.; Gonzalez, C.; Pople, J. A. *Gaussian 03*, rev. B.01 ed.; Gaussian, Inc.: Wallingford, CT, 2004.
(26) DeLuca, M. J.; Niu, B.; Johnson, M. A. *J. Chem. Phys.* **1988**, *88*, 5857.
(27) Johnson, M. A.; Lineberger, W. C. Pulsed Methods for Cluster Ion Spectroscopy. In *Techniques for the Study of Ion Molecule Reactions*; Farrar, J. M., Saunders, W. H., Eds.; Wiley: New York, 1988; p 591.
(28) Verlet, J. R. R.; Bragg, A. E.; Kammrath, A.; Cheshnovsky, O.; Neumark, D. M. *Science* **2005**, *307*, 93.
(29) Nauta, K.; Miller, R. E. *Science* **2000**, *287*, 293.

JP806478G